

PbTiO₃ addition and internal dynamics in Pb(Zn_{1/3}Nb_{2/3})O₃ crystal studied by Raman spectroscopy

Oleksiy Svitelskiy*

National High Magnetic Field Laboratory, Florida State University, Tallahassee, Florida 32310, USA

Duangmanee La-Orauttapong

Department of Physics-Science, Srinakharinwirot University, Bangkok 10110, Thailand

Jean Toulouse

Department of Physics, Lehigh University, Bethlehem, Pennsylvania 18015, USA

W. Chen and Z.-G. Ye

Department of Chemistry, Simon Fraser University, Burnaby, BC, Canada V5A 1S6

(Received 27 June 2004; revised manuscript received 10 October 2005; published 23 November 2005)

We present the results of the Raman study of lattice dynamics and development of mesoscopic range order in a relaxor ferroelectric Pb(Zn_{1/3}Nb_{2/3})O₃ crystal containing 4.5% of PbTiO₃ as it is cooling down from 1000 to 100 K. As in the other relaxors, the relaxor state develops in four stages separated by three temperatures: Burns temperature $\tilde{T}_B \sim 800$ K, intermediate temperature $T_d \sim 550$ K, and freezing temperature $T_f \sim 370$ K. However, the mixed crystal shows significant differences compared to the nominally pure one. First, there is a dramatic decrease of the scattered intensity above \tilde{T}_B ; second, a significant asymmetry of the polarizability tensor occurs near the T_d reflected by polarization properties of the central peak; third, a softening of line *B* (~ 780 cm⁻¹) is found in the neighborhood of T_d ; fourth, essentially different in each case is the splitting of the broad band *E* (~ 560 cm⁻¹), and its value can serve as an indicator of the order parameter in the system.

DOI: [10.1103/PhysRevB.72.172106](https://doi.org/10.1103/PhysRevB.72.172106)

PACS number(s): 77.80.-e, 78.30.-j, 63.20.Kr, 77.22.Gm

Although intensive exploration of the lead relaxors brought significant achievements,^{1,2} the lack of comprehensive studies of their Raman scattering is especially apparent. To fill this gap, we developed^{3,4} an approach to Raman analysis that allowed presenting a detailed picture of the thermal evolution of the internal dynamics and structural transformations in classical lead relaxors⁵ Pb(Mg_{1/3}Nb_{2/3})O₃ (PMN)³ and Pb(Zn_{1/3}Nb_{2/3})O₃ (PZN),⁶ while there are cooling down from 1000 to 100 K. In this paper, we concentrate on the Raman spectra of a PZN crystal, whose properties are modified by admixture of 4.5% PbTiO₃ (PT) in comparison to the nominally pure material. Understanding the influence of small additions of PT on the properties of lead relaxors is of particular importance, since these compositions are the most promising candidates for commercial usage.

The properties of lead relaxors are determined by their perovskite structure with ion off-centering and compositional inhomogeneities. At high temperature, the ions can move almost freely amongst equivalent off-center positions in the cell, so the crystal has an average $Pm\bar{3}m$ structure, in which 1:1 compositional clusters of $Fm\bar{3}m$ symmetry are present.⁷ With cooling down, the correlations between the neighboring cells increase. This increase can be considered as a process characterized by three temperatures:⁶ the Burns temperature, when the lifetime of polar fluctuations becomes big with respect to the inverse optical phonon frequency; an intermediate temperature T_d , when permanent polar nanoregions (PNR's) appear; and a freezing temperature T_f , when the

off-centered ions are locked in one position. Below T_f , the average correlation length constitutes $\sim 6-7$ nm in PMN⁸ and $\sim 15-20$ nm in PZN.⁹ Consequently, PMN preserves an average $Pm\bar{3}m$ symmetry down to the lowest temperatures, while PZN at temperature T_f undergoes transition to a microdomain $R3m$ state.^{10,11}

PT is a classical soft-mode ferroelectric. When admixed to the relaxor, it suppresses the relaxor properties and, if PT concentration is sufficiently high, causes the ferroelectric phase transition(s). On the phase diagram, the mixed PZN-4.5%PT composition is located halfway to the morphotropic phase boundary.¹² Consequently, its relaxor properties are influenced by the ferroelectric ones, but without spontaneous appearance of the long-range order.¹³ Application of electric field can induce a sequence of ferroelectric phase transitions.^{14,15}

We investigated polarized $\langle x|zz|y \rangle$ (VV) and depolarized $\langle x|zx|y \rangle$ (VH) Raman scattering of $\langle 100 \rangle$ cut single crystals. The PZN-4.5%PT crystal was grown by the top-cooling solution technique, using PbO flux.¹⁶ The reference PZN crystal was grown by a spontaneous nucleation from a high-temperature solution using an optimized flux composition of Pb and B₂O₃.¹⁷ Both crystals exhibited high optical quality. To ensure comparability of the results, all measurements were done in the same experimental conditions as described in Ref. 3.

The measured spectra were qualitatively consistent with the previously reported.¹⁸⁻²⁰ A typical PZN-4.5%PT spec-

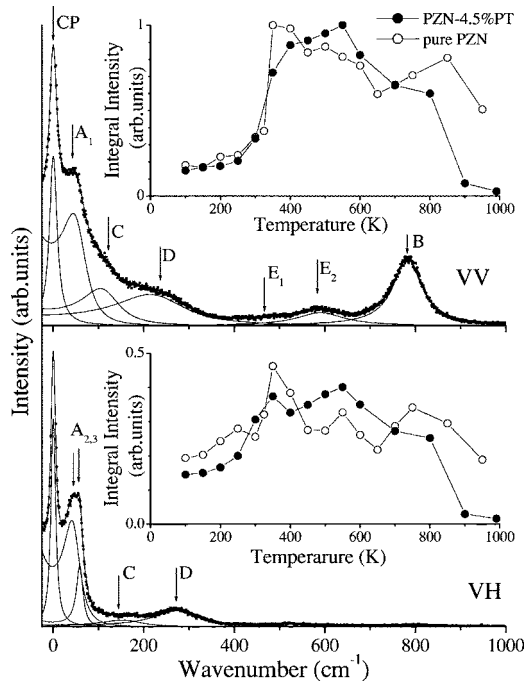


FIG. 1. Examples of PZN-4.5%PT Raman spectra at 400 K in VV and VH geometries. Solid lines demonstrate quality of the fit. Insets show temperature dependences of integral phonon scattering spectra for PZN-4.5%PT and PZN crystals.

trum (Fig. 1) consists of two strong lines centered approximately at 45 cm^{-1} (A) and 780 cm^{-1} (B), several weak and broad bands (C, D, and E), and of a central peak (CP). At first sight, these spectra as well as their thermal behavior are similar to those of nominally pure PZN.⁶ This suggests that the scattering in PZN-4.5%PT has first order character and originates from the regions of lower cubic symmetry,²¹ $Fm\bar{3}m$ and PNR's.²² It also implies that the lattice structure of PZN-4.5%PT has the same temperature trends of development as in the other relaxors. However, a careful look reveals dramatic changes caused by the influence of PT.

Insets to Fig. 1 show the temperature evolution of the integral intensities of the phonon contribution to VV (a) and VH (b) scattering spectra for both PZN-4.5%PT and PZN crystals. One can see that at high temperature the PZN-4.5%PT scattering intensity is very low in both VV and VH geometries (solid circles). It is also much lower than in PZN crystal (open circles). Lowering the temperature, at $\tilde{T}_B \sim 800 \text{ K}$, it sharply increases reaching the values comparable to those in PZN. The high-temperature drop of Raman intensity and the PT-induced decrease of the temperature when it occurs are often associated with high-temperature disappearance of the $Fm\bar{3}m$ clusters due to the thermal motion of ions²² and facilitation of this process by adding PT.¹⁹ In our opinion, the temperatures involved in this work are not sufficiently high for this explanation. At 1000 K some intersite diffusion of Mg and Nb ions is possible, but the time scale of this motion²³ is much slower than the time scale of our experiment. Alternatively, this effect can be explained by the changes in electronic and optical properties of the crystal.

With further cooling, the integral intensity in both geom-

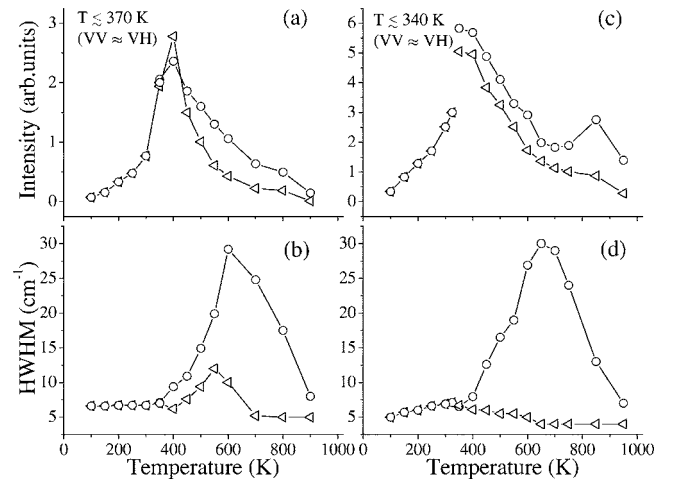


FIG. 2. Fitted parameters of the CP in PZN-4.5%PT (left) and PZN (right) crystals. Intensities are presented in (a) and (c), half widths at half maxima are shown in (b) and (d).

etries monotonically increases until it reaches maximum at $T_d \sim 550 \text{ K}$. Transition to microdomain state at $T_f \sim 370 \text{ K}$ is marked by loss of polarization information (VV and VH spectra become almost equal) and a decrease of the scattered intensity. These effects are caused by the multiple scattering on the walls of PNR's, when their size is comparable to the wavelength of light.¹⁰ A smoothness of the transition at T_f in PZN-4.5%PT, comparatively to PZN, is not surprising, considering that the x-ray data¹⁴ suggest a sequence of local phase transformations around this temperature.

The spectra were decomposed into a number of peaks using procedure described in Ref. 3. To ensure detection of the finest details, VV and VH components for both PZN-4.5%PT and PZN were fitted separately. The central peak (CP) was approximated by Lorentzian, the phonon peaks were described as damped harmonic oscillators multiplied by the Bose factor. The quality of the fit is shown in Fig. 1. For PZN, the current results were consistent with the earlier ones,⁶ confirming the characteristic temperatures of its thermal evolution, $T_B^{PZN} \sim 650 \text{ K}$, $T_d^{PZN} \sim 450 \text{ K}$, and $T_f^{PZN} \sim 340 \text{ K}$. For PZN-4.5%PT, the fitting helped us to determine these temperatures: $\tilde{T}_B \sim 800 \text{ K}$, $T_d \sim 550 \text{ K}$, and $T_f \sim 370 \text{ K}$, and revealed a number of differences from PZN.

In Raman spectrum, a CP can be caused either by relaxational dynamics,^{24,25} or by zone-center softening of the transverse-optical (TO) phonon,²⁶ or by interaction of these two processes.²⁷ The common for relaxors overdamping of the zone center TO phonon²⁸ suggests relaxational origin of the CP. When relaxations are fast,²⁹ the CP is nonintense and broad. Their slowing down causes growth and narrowing of the peak. A similarity in the temperature behavior of the CP in PZN-4.5%PT and PZN crystals (Fig. 2) with those of PMN³ and KTN⁴ suggests applicability of the model,^{3,4,30} explaining CP by the relaxational motion of the PNR's and its progressive restriction with decreasing temperature: from possibility of almost free reorientational motion at high temperature, down to confinement in a single direction at low temperature. However, such a parallel should be drawn with caution. In KTN the main ferroelectric ion is (111)-shifted

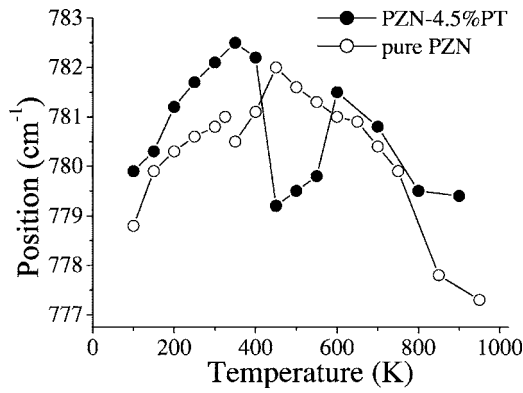


FIG. 3. Position of the line B in PZN-4.5%PT and PZN.

Nb,³¹ and in the lead relaxors the highest shift is of spherically distributed Pb ions.^{32,33} With cooling down, in all these materials the growing correlations cause development of the lower symmetry polar clusters.^{7-9,33}

Figure 2(a) shows that with cooling the crystal, below $\tilde{T}_B \sim 800$ K, the intensity of the PZN-4.5%PT CP increases, pointing out the appearance of restrictions on relaxational motion of ions and nucleation of slowly (with respect to the optical phonon frequency⁶) relaxing fluctuations. In PZN [Fig. 2(c)] and PMN,³ the beginning of such an increase marks the Burns temperature, accompanied by the deviation of the refraction index,³⁴ the TO phonon overdamping,²⁸ and a soft mode.³⁵ The presence of the TO phonon overdamping in the low PT concentration PZN-PT³⁶ supports the possible existence of the Burns temperature in it. However, the onset of the high-temperature decrease of the scattered intensity disrupts the exact determination of its value from the Raman data. Therefore, we use the tilde over \tilde{T}_B . Below $T_d \sim 550$ K the width of the CP [Fig. 2(b)] decreases, pointing out further slowing down of the relaxations; simultaneous appearance of the diffuse neutron scattering³⁷ allows us to associate T_d with nucleation of the “permanent” PNR’s. Unlike PZN [Fig. 2(d)], in PZN-4.5%PT [Fig. 2(b)], the width of the CP exhibits broadening in both VV and VH geometries, implying an anisotropy of the polarizability tensor²¹ (e.g., presence of the time-averaged monoclinic distortions³³). Below $T_f \sim 370$ K the CP is narrow and its intensity decreases, pointing out the formation of the network of “static” rhombohedral clusters.¹²

The most sensitive to the 4.5%PT addition are the high-energy peaks B and E . The peak B of A_{1g} symmetry originates from the breathing vibrations of oxygen octahedra.³⁸ It is known to be responsive to the subtle changes in the lattice structure.²² Figure 3 shows that adding PT causes its softening around $T_d \sim 550$ K.

The band E of E_g symmetry is related to TO_4 vibration.³⁹ In PMN,³ at high temperature this band was broad and weak; with cooling it became a doublet, and its intensity was growing. The temperature dependence of the distance between components was following a characteristic order parameter behavior, suggesting the existence of a latent phase transformation. A similar behavior was also observed in some lead zirconate ceramics.⁴⁰

Unlike the case of PMN, in PZN band E [Fig. 4(a)] con-

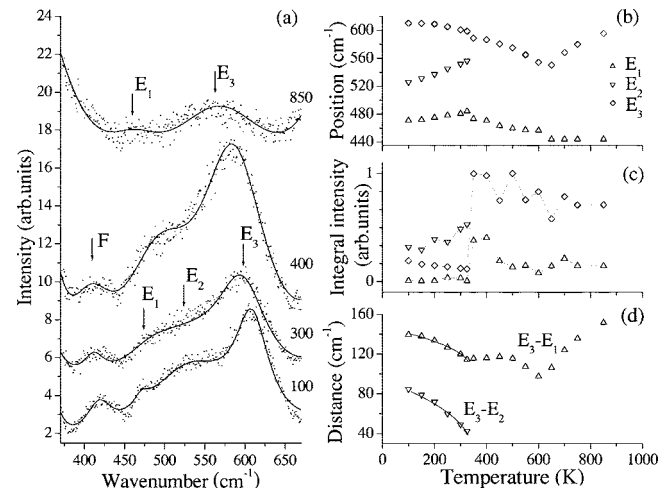


FIG. 4. Peak E in PZN. (a) examples at several temperatures, solid lines show quality of the fit; positions (b) and integral intensities (c) of the peak components. Distances between them (d) demonstrate that splitting follows the critical dependence law, solid lines represent $(T_f^{PZN} - T)^{1/2}$ fit.

sists of two components, E_1 and E_3 , even at as high temperature as 850 K. Below T_f^{PZN} , a component E_2 appears. The temperature dependences of the parameters of these three components [Figs. 4(b)–4(d)] are very sensitive to the processes in the crystal. Below $T_f^{PZN} \sim 340$ K, the distances $E_3 - E_1$ and $E_3 - E_2$ both follow a $(T_f^{PZN} - T)^{-1/2}$ law, suggesting that in our crystals, such as in the case of CaAlNbO_3 ,⁴¹ line E follows the development of the order parameter. In PZN-4.5%PT (Fig. 5) at high temperature, line E is presented by a single component E_2 . At $T_f \sim 370$ K, a component E_1 appears. The distance between E_1 and E_2 remains almost constant down to the lowest measured temperature. Unlike PZN, in PZN-4.5%PT there is no third component of line E [Figs. 5(b) and 5(c)]. The origin of the splitting is still not quite understood. The high-frequency component might be originating from asymmetric breathing of the oxygen oc-

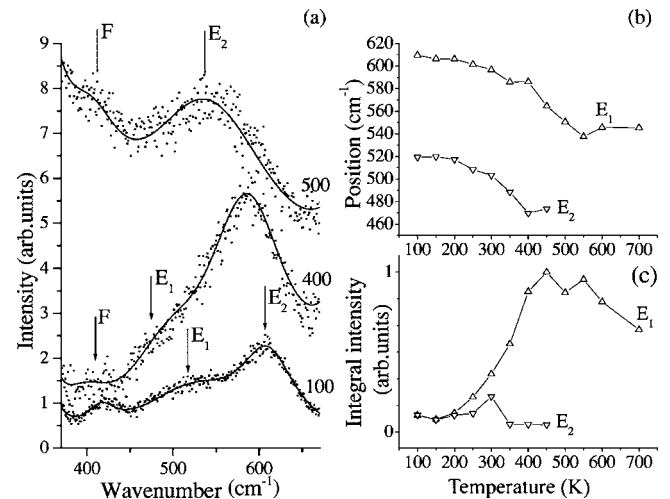


FIG. 5. Peak E in PZN-4.5%PT: (a) examples at several temperatures, solid lines show quality of the fit; positions (b) and integral intensities (c) of the peak components.

tahedra, and the other two from oscillations of oxygen ions in directions perpendicular to the Mg-O-Nb line.^{41,42}

In summary, as in the other relaxors, in PZN-4.5%PT the development of the low-temperature state is a process marked by three characteristic temperatures related to the slowing of the polar fluctuations, appearance of PNR's, and freezing of their motion. Also, Raman spectra are sensitive to individual properties of the crystal. The high-temperature (above $\tilde{T}_B \sim 800$ K) intensity decrease reflects changes in the optical properties of the sample. Evolution of the central

peak points out an asymmetry of the polarizability tensor at temperatures around $T_d \sim 550$ K. The phonon peak B (~ 780 cm⁻¹) shows softening towards this temperature. The thermal evolution of the broad band E (~ 560 cm⁻¹) in different relaxors goes differently. The appearance of the low-temperature order at $T_f \sim 370$ K is reflected in the splitting of this line.

Many thanks to S. Prosandeev, G. Yong, V. Dierolf, A. Souslov, E. Venger, and G. Semenova for stimulating discussions.

*On leave from the Institute of Semiconductor Physics, Kyiv 03028, Ukraine.

- ¹G. Shirane, G. Xu, and P. M. Gehring, Conference Proc. for the NATO Advanced Research Workshop on the Disordered Ferroelectrics, Kiev, May 2003 [Ferroelectrics **321**, 7 (2005)].
- ²Z. G. Ye, Key Eng. Mater. **155-156**, 81 (1998).
- ³O. Svitelskiy, J. Toulouse, G. Yong, and Z.-G. Ye, Phys. Rev. B **68**, 104107 (2003).
- ⁴O. Svitelskiy and J. Toulouse, J. Phys. Chem. Solids **64**, 665 (2003).
- ⁵P. M. Gehring, W. Chen, Z.-G. Ye, and G. Shirane, cond-mat/0304289 (unpublished).
- ⁶J. Toulouse, F. Jiang, O. Svitelskiy, W. Chen, and Z.-G. Ye, Phys. Rev. B **72**, 184106 (2005).
- ⁷D. M. Fanning, I. K. Robinson, X. Lu, and D. A. Payne, J. Phys. Chem. Solids **61**, 209 (2000).
- ⁸I.-K. Jeong, T. W. Darling, J. K. Lee, Th. Proffen, R. H. Heffner, J. S. Park, K. S. Hong, W. Dmowski, and T. Egami, cond-mat/0412173 (unpublished).
- ⁹D. La-Orautapong, J. Toulouse, J. L. Robertson, and Z.-G. Ye, Phys. Rev. B **64**, 212101 (2001).
- ¹⁰A. Lebon, M. El Marssi, R. Farhi, H. Dammak, and G. Calvarin, J. Appl. Phys. **89**, 3947 (2001).
- ¹¹L. S. Kamzina, N. N. Krainik, L. M. Sapozhnikova, and S. V. Ivanova, Sov. Phys. Solid State **33**, 1169 (1991).
- ¹²D. La-Orautapong, B. Noheda, Z.-G. Ye, P. M. Gehring, J. Toulouse, and D. E. Cox, G. Shirane, Phys. Rev. B **65**, 144101 (2002).
- ¹³G. A. Samara, E. L. Venturini, and V. H. Schmidt, Phys. Rev. B **63**, 184104 (2001).
- ¹⁴A.-E. Renault, H. Dammak, G. Calvarin, P. Gaucher, and M. P. Thi, J. Appl. Phys. **97**, 044105 (2005).
- ¹⁵M. Shen and W. Cao, J. Appl. Phys. **95**, 8124 (2004).
- ¹⁶W. Chen and Z.-G. Ye, J. Mater. Sci. **36**, 4393 (2001).
- ¹⁷L. Zhang, M. Dong, and Z.-G. Ye, Mater. Sci. Eng., B **78**, 96 (2000).
- ¹⁸F. Jiang and S. Kojima, Jpn. J. Appl. Phys., Part 1 **38**, 5128 (1999).
- ¹⁹M. Iwata, N. Tomisato, H. Orihara, H. Ohwa, N. Yasuda, and Y. Ishibashi, Ferroelectrics **261**, 83 (2001).
- ²⁰S. Gupta, R. S. Katiyar, R. Guo, and A. S. Bhalla, J. Raman Spectrosc. **31**, 921 (2000).
- ²¹D. A. Long, *Raman Spectroscopy* (McGraw-Hill, New York, 1977).
- ²²I. G. Siny, S. G. Lushnikov, R. S. Katiyar, and V. H. Schmidt, Ferroelectrics **226**, 191 (1999).
- ²³M. A. Akbas and P. K. Davies, J. Am. Ceram. Soc. **83**, 119 (2000).
- ²⁴I. G. Siny, S. G. Lushnikov, R. S. Katiyar, and E. A. Rogacheva, Phys. Rev. B **56**, 7962 (1997).
- ²⁵J. P. Sokoloff, L. L. Chase, and D. Rytz, Phys. Rev. B **38**, 597 (1988).
- ²⁶M. D. Fontana, G. E. Kugel, and C. Carabatos-Nedelec, Phys. Rev. B **40**, 786 (1989).
- ²⁷B. E. Vugmeister, Y. Yacoby, J. Toulouse, and H. Rabitz, Phys. Rev. B **59**, 8602 (1999).
- ²⁸P. M. Gehring, S.-E. Park, and G. Shirane, Phys. Rev. B **63**, 224109 (2001).
- ²⁹K. H. Michel, J. Naudts, and B. De Raedt, Phys. Rev. B **18**, 648 (1978).
- ³⁰G. Yong, J. Toulouse, R. Erwin, S. M. Shapiro, and B. Hennion, Phys. Rev. B **62**, 14736 (2000).
- ³¹O. Hanske-Petitpierre, Y. Yacoby, J. Mustre de Leon, E. A. Stern, and J. J. Rehr, Phys. Rev. B **44**, 6700 (1991).
- ³²K. Hirota, Z.-G. Ye, S. Wakimoto, P. M. Gehring, and G. Shirane, Phys. Rev. B **65**, 104105 (2002).
- ³³B. Dkhil, J. M. Kiat, G. Calvarin, G. Baldinozzi, S. B. Vakhru-shev, and E. Suard, Phys. Rev. B **65**, 024104 (2001).
- ³⁴G. Burns and F. H. Dacol, Solid State Commun. **48**, 853 (1983); Phys. Rev. B **28**, 2527 (1983).
- ³⁵S. B. Vakhrushev and S. M. Shapiro, Phys. Rev. B **66**, 214101 (2002).
- ³⁶P. M. Gehring, S.-E. Park, and G. Shirane, Phys. Rev. Lett. **84**, 005216 (2000).
- ³⁷D. La-Orautapong, J. Toulouse, Z.-G. Ye, W. Chen, R. Erwin, and J. L. Robertson, Phys. Rev. B **67**, 134110 (2003).
- ³⁸E. Husson, L. Abello, and A. Morell, Mater. Res. Bull. **25**, 539 (1990).
- ³⁹S. Kamba, E. Buixaderas, J. Petzelt, J. Fousek, J. Nosek, and P. Bridenbaugh, J. Appl. Phys. **93**, 933 (2003).
- ⁴⁰M. El. Marssi, R. Farhi, X. Dai, A. Morell, and D. Viehland, J. Appl. Phys. **80**, 1079 (1996).
- ⁴¹I. Levin, S. A. Prosandeev, and J. E. Maslar, Appl. Phys. Lett. **86**, 011919 (2005); S. A. Prosandeev, U. Waghmare, I. Levin, and J. Maslar, Phys. Rev. B **71**, 214307 (2005).
- ⁴²S. A. Prosandeev, E. Cockayne, B. P. Burton, S. Kamba, J. Petzelt, Yu. Yuzyuk, R. S. Katiyar, and S. B. Vakhru-sev, Phys. Rev. B **70**, 134110 (2004).